

# Simulating Dirac equation with Josephson junction circuits

Xiao hui Ji,<sup>1,2,\*</sup> Wen bin Lin,<sup>3</sup> Jia gang Zeng,<sup>3</sup> and Guang di Wang<sup>4</sup>

<sup>1</sup>*School of Materials and Engineering, Southwest jiaotong University Chengdu 610031, PR China*

<sup>2</sup>*Key Laboratory of Advanced Technology for Materials of Education Ministry, Southwest jiaotong University Chengdu 610031, PR China*

<sup>3</sup>*School of Physical Science and Technology, Southwest Jiaotong University, Chengdu 610031, China*

<sup>4</sup>*School of Civil Engineering, Southwest Jiaotong University, Chengdu 610031, China*

(Dated: June 15, 2018)

We propose a scheme for simulating 3+1, 2+1, 1+1 Dirac equation for a free spin-1/2 particle with superconducting Josephson junctions consisting of five qubits, four qubits, two qubits respectively. In 3+1D and 2+1D, the flux qubit1 driven by a resonant pulse is in the superposition state of its own two eigenstates, and it is used as a bus to induce the (blue)red-sideband excitation consisting of a magnetic pulse acting resonantly on two levels of the flux qubit2 and the energy levels of one phase qubit, which yields two (Anti)Jaynes-Cummings interactions with one driving pulse and reduces the damage of the driving pulses to the system consequently. Numerical results show that decoherence time is several times longer than transition time supposing set appropriate experimental parameters. Therefore experiments verifying the dynamics of electron and neutrino, such as *Zitterbewegung* effect in 3+1, 2+1 and 1+1 dimensions, can be implemented by microelectronic chips composed of the qubits as artificial atoms.

Due to the importance of Dirac equations, the simulations of Dirac equation are attracting more attentions. The pioneering schemes for the 1+1 and 3+1 Dirac equation in trap ion system are proposed in 2007 [1, 2]. The 1+1 Dirac equation has been experimentally implemented in trapped ions system and the corresponding *Zitterbewegung* effect has been observed [3]. The propagations of photon in 2D photonic crystals and acoustic wave in the 2D sonic crystals obey the 2+1 Dirac equation for  $m=0$  and spin-1 and the Dirac tremor has been found to occur at the Dirac point of the crystals [4, 5]. However, there is no experimental simulation for the 3+1 Dirac equation for a spin-1/2 particle so far.

Inspired by the original ideas that Josephson junctions circuits simulate natural atom [6, 7] and the trapped ions simulate the Dirac equations [1-3, 8, 9], in this *Letter* we propose a convenient scheme for simulating the 3+1, 2+1, and 1+1 Dirac equation based on the superconducting Josephson junctions circuits. Josephson devices can behave like artificial atoms [6, 7], meanwhile possess new features [10]. Under the present low temperature and the fabrication technology, Josephson devices have been used widely in the fields of quantum information [11] and quantum simulation [12, 13].

The proposed scheme is based on the unified description of *Zitterbewegung* effect [9]. The circuit diagram is shown in Fig. 1. The 3+1D, 2+1D and 1+1D simulations can be implemented with the structures of five qubits, four qubits, two qubits respectively. The levels of magnetic flux qubits are mapped to the positive and negative energy levels, and the two spin levels of the particle. The particle momentum in each dimension corresponds to a phase qubit, and the momentum operator in every dimension is proportional to the translational operator constructed by the phase of its corresponding phase qubit. Fig. 2 presents the simulation results for the observations and the suggested parameters of the circuits.

Here, we focus on the mutual coupling caused by the shared junction and the self-coupling is written directly. The phase constraint conditions in the  $l$ th flux qubit loop and in  $p$ th phase qubit loop give

$$\begin{aligned} 2\pi f_1^{(l)} + \varphi_1^{(l)} + \varphi_2^{(l)} + \varphi_3^{(l)} + \varphi_r^{(l)} + \sum_{i=r_l} \Phi_i^{(l)} &= 0 \\ \varphi_r^{(l)} = \varphi_L^{(l)} + (-1)^l \gamma_O + \sum_P \gamma_P, \quad \varphi_4^{(l)} - \varphi_3^{(l)} + 2\pi f_2^{(l)} &= 0 \\ \varphi_p + \varphi_{Lp} - \gamma_P + 2\pi f_p &= 0 \end{aligned}$$

where lowercase  $p$  corresponds to uppercase  $P$ ; 3+1D:  $r_l=1, 2, 3$ ;  $l=1:P=X, Z$ ;  $l=2:P=Y$ . 2+1D:  $r_l=1, 2$ ;  $l=1:P=X$ ;  $l=2:P=Y$ . 1+1D:  $r_l=1, 2$ ;  $\gamma_O=0$ ;  $l=1:P=X$ . To be simplified, the dynamics of the models representing 3+1, 2+1, 1+1 Dirac equations can be generally written as the Hamiltonian

$$H = \sum_{l=L} H_q^{(l)} + \sum_{p=c} H_p + \sum_{P=C} H_P + \sum_{pP} H_{pP} + H_O \quad (1)$$

\*Electronic address: xiaohui.cc.ji@gmail.com

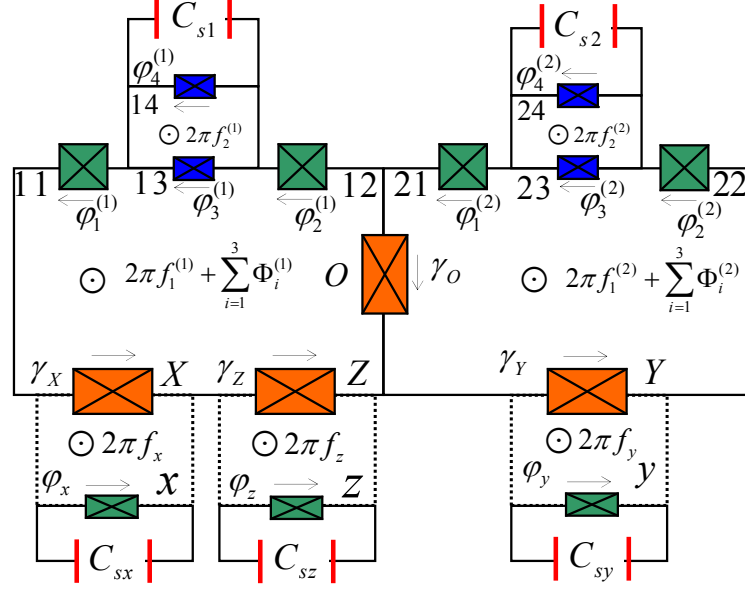


FIG. 1: (color online) Electrical schematic of the 3D Dirac equation simulations. E-mail icon ( $\times$  in  $\square$ ) represents the Josephson junctions (JJ). The black solid and dotted lines represent the superconductive wires. The  $l$ th flux qubit consists of JJ  $l1$  (green),  $l2$  (green),  $l3$  (blue),  $l4$  (blue) and the superconductivity wires with inductance  $L_g^{(l)}$ . Here  $l = 1$  or  $2$ . Both JJ  $l1$  and  $l2$  have Josephson energy  $E_J^{(l)}$  and capacitance  $C_J^{(l)}$ , and JJ  $l3$  and  $l4$  are smaller than  $l1$  (or  $l2$ ) by a factor  $\alpha_l$ . The loop enclosing JJ  $l1$ ,  $l2$  and  $l3$  is applied with the reduced flux  $2\pi f_1^{(l)}$  and the weak time-dependent magnetic fluxes  $\Phi_i^{(l)}$  (driving pulse), where  $\Phi_i^{(l)} = n_i^{(l)} \cos(\omega_i^{(l)} t + \phi_i^{(l)})$ ,  $i = 1, 2, 3$ .  $\varphi_i^{(l)}$  denotes the phase differences across  $i$ th junction in  $l$ th qubit loop and  $\varphi_L^{(l)}$  is the phase differences due to the inductance of superconductivity ring in  $l$ th qubit loop. The SQUID loop, consisted of JJ  $l3$  and  $l4$  which are parallel to the capacitor  $C_{s1}$  (red), is biased by the reduced flux  $2\pi f_2^{(l)}$ . The shunt capacitance  $C_{s1}$  is  $(\beta_l - 2\alpha_l)$  times of Josephson junction capacitance. The two flux qubits couple to each other with the shared large Josephson junction  $O$  (orange) which has Josephson energy  $E_{JO}$  and capacitance  $C_{JO}$ . The phase qubit  $p$ , parallel to a single crystal silicon capacitor  $C_{sp}$  (red), has Josephson energy  $E_{JP}$  and capacitance  $C_{JP}$ , and the shared large junction  $P$  has Josephson energy  $E_{JP}$  and capacitance  $C_{JP}$ . Here  $p = x, y, z$  and  $P = X, Y, Z$ . The Josephson energies satisfy  $E_{JP}, E_{JO} \gg E_J^{(l)}, E_{JP}$ . The loop, containing the phase qubit  $p$ , the shared large junction  $P$  and the superconductivity wire (the dotted line) with inductance  $L_p$ , is applied with the reduced flux  $2\pi f_p$ , which provides a current offset for the phase qubit  $p$ .  $\varphi_p, \gamma_O, \gamma_P$  denote the phase differences across the phase qubit  $p$ , shared junction  $P$ , shared junction  $O$  and  $\varphi_{Lp}$  is the phase differences due to the inductance  $L_p$ . All of the shared junctions in the scheme can be replaced by the superconducting wires with the same inductive values. The first flux qubit ( $l = 1$ ) interacts with the phase qubits  $p = x, z$  (green) with the shared large Josephson junctions  $P = X, Z$  (orange), and the second flux qubit ( $l = 2$ ) interacts with the phase qubit  $p = y$  (green) with the shared large Josephson junction  $P = Y$  (orange). This 3D electrical schematic reduces to the 2D electrical schematic by removing the loop containing the phase qubit  $z$ , the shared large junction  $Z$ , and further reduces to the 1D case by removing the second flux qubit ( $l = 2$ ) and the shared large Josephson junction  $O$  (orange).

$$\begin{aligned}
3+1D : L &= 2; C = X, Y, Z; c = x, y, z; \\
pP : p &= x \& P = X; p = y \& P = Y; p = z \& P = Z; \\
2+1D : L &= 2; C = X, Y, T; c = x, y, z; \\
pP : p &= x \& P = X; p = y \& P = Y; \\
1+1D : L &= 1; C = X; c = x; H_O = 0; pP : p = x \& P = X.
\end{aligned}$$

Here,  $H_q^{(l)}$  in equation(1) is the Hamiltonian of single flux qubit [14, 15, 17–20], and it is shown as

$$\begin{aligned}
H_q^{(l)} &= 2E_{C_a}^{(l)} N_{al}^2 + 2E_{C_s}^{(l)} N_{sl}^2 - 2E_J^{(l)} \cos \varphi_a^{(l)} \cos \varphi_s^{(l)} \\
&\quad - 2\alpha_l E_J^{(l)} \cos(\pi f_2^{(l)}) \cos(2\varphi_s^{(l)} + 2\pi f_3^{(l)} + \varphi_r^{(l)} + \sum_{i=1}^3 \Phi_i^{(l)}) \\
&\quad + [2\beta_l / (1 + 4\beta_l)] \hbar N_s^{(l)} \sum_{i=1}^3 \dot{\Phi}_i^{(l)} + \frac{1}{2} L_r^{(l)} [I^{(l)}]^2
\end{aligned}$$

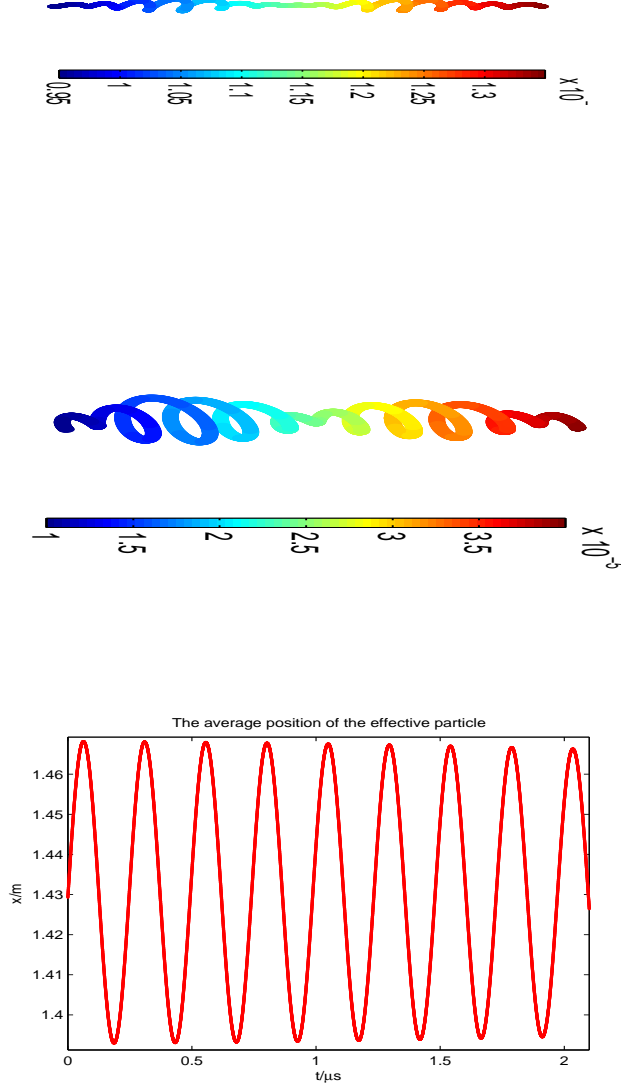


FIG. 2: The results similar to that shown in figure can be obtained by observing the circuits in Fig 1. In the figure, the average position of ion with spin 1/2, rest mass  $m \neq 0$  and  $m = 0$  are given respectively. The top graph shows  $m \neq 0$  particles' 3+1 dimensional average position, the middle graph represents  $m = 0$  particles' 3+1 dimensional average position, the bottom graph depicts  $m \neq 0$  particles' 1+1 dimensional average position.  $E_J^{(1)}/h = 300GHz$ ,  $E_J^{(2)}/h = 400GHz$ ,  $E_C^{(1)} = e^2/(2C_J^{(1)})$ ,  $E_C^{(2)} = e^2/(2C_J^{(2)})$ ,  $E_J^{(1)}/E_C^{(1)} = 30$ ,  $E_J^{(2)}/E_C^{(2)} = 30$ ,  $\beta_1 \sim 6$ ,  $\beta_2 \sim 6$ ,  $\alpha_1 = 0.6$ ,  $\alpha_2 = 0.6$ ,  $f_1^{(1)} = f_1^{(2)} \in [1/3 + \Delta f/2 - 0.2, 1/3 + \Delta f/2 + 0.2]$ ,  $f_2^{(1)} = f_2^{(2)} = 1/3 - \Delta f$ ,  $\Delta f = 0.015$ , The stable region: qubit1  $f_1^{(1)} + \Delta f/2 \pm 0.02$ ; qubit2  $f_1^{(2)} + \Delta f/2 \pm 0.2$ . geometric inductance  $L_g^{(1)} \sim 33pH$ ,  $L_g^{(2)} \sim 33pH$ ,  $\Lambda_1 = L_r^{(1)}/L_J^{(1)} \sim 0.17$ ,  $\Lambda_2 = L_r^{(2)}/L_J^{(2)} \sim 0.23$ ,  $L_r^{(l)} = L_g^{(l)} + \sum_P L_{JP} + L_{JO}$ . Where,  $l = 1$  and  $P = X, Z$ ,  $l = 2$  and  $P = Y$  in 3+1 dimension;  $l = 1$  and  $P = X$ ,  $l = 2$  and  $P = Y$  in 2+1 dimension;  $L_{JO} = 0$  and  $P = X$  in 1+1 dimension.  $L_{Jp}$ ,  $L_{JP}$ ,  $L_{JO}$  denote effective inductance of phase qubit  $p$ , shared junction  $P$ , shared junction  $O$  respectively. The phase qubit parameter:  $p = x, y, z$ ,  $P = X, Y, Z$ ;  $E_{Jp}/h = 850 \sim 1350GHz$ ,  $f_p$  is set properly so that  $\sin \varphi_{p0} = I_{pb}/I_{p0} = 0.99$ ,  $I_{pb}$  bias current,  $I_{p0}$  critical current.  $E_{Jp}/E_{Cp} = 10^{-6}$ ,  $E_{Cp} = e^2/(C_{Jp} + C_{sp})$ ,  $E_{Lp} = (\Phi_0/2\pi)^2/(2L_p)$ , the total inductance of the ring enclosing the phase qubit  $p$  and shared junction  $P$  is  $L_{rp} = L_p + L_{JP}$ , geometric inductance  $L_p \sim 40pH$ . All shared junction are biased by no current source. The shared junction parameter:  $E_{JP}/h \sim 8000GHz$ ,  $\varphi_{P0} = \arcsin(I_{Pb}/I_{P0})$ ,  $I_{Pb}$  bias current,  $I_{P0}$  critical current.  $E_{JO}/h \sim 8000GHz$ ,  $\varphi_{O0} = \arcsin(I_{Ob}/I_{O0})$ ,  $I_{Ob}$  bias current,  $I_{O0}$  critical current.  $n_x, n_y, n_z \sim 0.005 - 0.025$ , weak radio-frequency field  $\Phi_i^{(l)} \sim 0.005 - 0.025\Phi_0$ .  $mc^2$  the rest energy of ion,  $cp$  the kinetic energy. 3+1D and 2+1D:  $mc^2 = 0 \sim 5MHz$ ,  $cp = 0.02 \sim 0.1MHz$ ; 1+1D:  $mc^2 = 1 \sim 5MHz$ ,  $cp = 0.01 \sim 10MHz$

The circling current is shown as [14, 15, 17–22]

$$I^{(l)} = (2e)(\dot{N}_{sl} + \dot{N}_{al}) + (2\pi/\Phi_0)E_J^{(l)} \sin(\varphi_s^{(l)} + \varphi_a^{(l)})$$

charging energy  $E_{Ca}^{(l)} = e^2/2C_J^{(l)}$ ,  $E_{Cs}^{(l)} = e^2/[2C_J^{(l)}(1 + 4\beta_l)]$ , cooper pair operator  $N_{al} = -i\partial/\partial\varphi_a^{(l)}$ ,  $N_{sl} = -i\partial/\partial\varphi_s^{(l)}$ , new phase variables  $\varphi_a^{(l)} = (\varphi_1^{(l)} - \varphi_2^{(l)})/2$ ,  $\varphi_s^{(l)} = (\varphi_1^{(l)} + \varphi_2^{(l)})/2$ , flux bias  $f_3^{(l)} = f_1^{(l)} + f_2^{(l)}/2$ ,  $\Phi_0$  magnetic flux quantum.  $\hbar = h/2\pi$ ,  $h$  is planck constant.  $e$  is electronic charge. Here,  $H_p$  in equation(1) is the Hamiltonian of  $p$ th phase qubit, and it is described as [21]

$$H_p = 4E_{cp}N_p^2 - E_{Jp}(\cos \varphi_p + I_{pb}\varphi_p/I_{p0}) + E_{rp}(\varphi_p - \varphi_{p0})^2/2$$

charging energy  $E_{cp} = e^2/2(C_p + C_{sp})$ , cooper pair operator  $N_p = -i\partial/\partial\varphi_p$ , the coupling energy  $E_{rp} = (\Phi_0/2\pi)^2/L_{rp}$ . Here,  $H_P$  in equation(1) is the Hamiltonian of  $P$ th shared phase junction, and it is described as[18, 21]

$$H_P = (\Phi_0/2\pi)^2 C_P \dot{\gamma}_P^2/2 - E_{JP}(\cos \gamma_P + I_{Pb}\gamma_P/I_{P0})$$

Here,  $H_{pP}$  in equation(1) is the Hamiltonian of superconducting ring corresponding  $p$ th phase qubit and shared junction  $P$ , and it is described as [21]

$$H_{pP} = (E_{Lp}/2)(\varphi_p - \gamma_P + 2\pi f_p)^2$$

The effective coupling energy is  $E_{Lp} = (\Phi_0/2\pi)^2/L_p$ . Here,  $H_O$  in equation(1) is the Hamiltonian of  $O$ th big phase junction, and it is described as[18, 21]

$$H_O = (\Phi_0/2\pi)^2 C_O \dot{\gamma}_O^2/2 - E_{JO} \cos \gamma_O + I_{Ob}\gamma_O/I_{O0}$$

$H_{q0}^{(l)}$  indicates the Hamiltonian of the  $l$ th bare magnetic flux qubit biased by the static magnetic field.  $|e_l\rangle$ ,  $|g_l\rangle$  represent two lower energy eigenstates of  $H_{q0}^{(l)}$ . For convenience, the basis spaces  $\{|g_1\rangle, |e_1\rangle\}$ ,  $\{|g_2\rangle, |e_2\rangle\}$  are transformed respectively into  $\{|1D\rangle, |1U\rangle\}$ ,  $\{|20\rangle, |21\rangle\}$ ,  $H_{q0}^{(1)}$ ,  $H_{q0}^{(2)}$  are transformed respectively into

$$H_{D0}^{(1)} = \hbar X_0^{(1)} \hat{\sigma}_x^{(1)}, \quad H_{D0}^{(2)} = \hbar Z_0^{(2)} \hat{\sigma}_z^{(2)}.$$

The Pauli operators are defined by

$$\hat{\sigma}_z = \begin{pmatrix} 1 & 0 \\ 0 & -1 \end{pmatrix} \quad \hat{\sigma}_x = \begin{pmatrix} 0 & 1 \\ 1 & 0 \end{pmatrix} \quad \hat{\sigma}_+ = \begin{pmatrix} 0 & 1 \\ 0 & 0 \end{pmatrix} \quad \hat{\sigma}_- = \begin{pmatrix} 0 & 0 \\ 1 & 0 \end{pmatrix}$$

In population representation, the Hamiltonian  $H_p$  and photon energy are shown as

$$H_p = \hbar\omega_p(\hat{a}_p^+ \hat{a}_p + 1/2), \quad \hbar\omega_p = [8E_{cp}(E_{Jp} \cos \varphi_{p0} + E_{rp})]^{1/2}$$

The boson operator is shown as

$$\hat{a}_p^+ = \varphi_{p1}/(2\lambda_p) - i\lambda_p N_p, \quad \lambda_p = [2E_{cp}/(E_{Jp} \cos \varphi_{p0} + E_{rp})]^{1/4}$$

$|n_p\rangle$  represent eigenstates of  $p$  phase qubit[21]. Similarly, the Hamiltonian of the shared junction

$$H_P = \hbar\omega_P \hat{a}_P^+ \hat{a}_P, \quad H_O = \hbar\omega_O \hat{a}_O^+ \hat{a}_O$$

Rotating frame by reference

$$H = \sum_{l=L} H_{D0}^{(l)} + \sum_{p=c} H_p + \sum_{P=C} H_P + H_O \quad (2)$$

satisfying the conditions of the frequencies

$$\begin{aligned} +2X_0^{(1)} - \omega_3^{(1)} &= 0, \quad \phi_3^{(1)} = 0, \quad n_3^{(1)} = n_m \\ +\omega_z - \omega_3^{(2)} &= 0, \quad \phi_3^{(2)} = -\pi/2, \quad n_3^{(2)} = n_z \\ +2Z_0^{(2)} + \omega_y - \omega_1^{(1)} &= 0, \quad \phi_1^{(1)} = 0, \quad n_1^{(1)} = n_y \\ +2Z_0^{(2)} - \omega_y - \omega_2^{(1)} &= 0, \quad \phi_2^{(1)} = \pi, \quad n_2^{(1)} = n_y \\ +2Z_0^{(2)} + \omega_x - \omega_1^{(2)} &= 0, \quad \phi_1^{(2)} = -\pi/2, \quad n_1^{(2)} = n_x \\ +2Z_0^{(2)} - \omega_x - \omega_2^{(2)} &= 0, \quad \phi_2^{(2)} = +\pi/2, \quad n_2^{(2)} = n_x \\ \omega_O \gg \omega_X \neq \omega_Y \neq \omega_Z &\gg 2X_0^{(1)}, 2Z_0^{(2)}, \omega_i^{(l)} \end{aligned}$$

then the iterative calculations are carried out according to the following formula

$$U = 1 + \sum_{n=1}^{\infty} \left(\frac{-i}{\hbar}\right)^n \int_{t_0}^t dt_1 \cdots \int_{t_0}^{t_{n-1}} H_I(t_1) \cdots H_I(t_n) dt_n \quad (3)$$

Establish mapping relationship between two systems:

$$\begin{aligned}
c &\sim 2\Delta_p \tilde{\Omega}_p, \quad \Delta_p = \lambda_p, \quad \hat{p}_p = i\hbar(a_p^+ - a_p^-)/2\Delta_p \\
c\hat{p}_p &\sim \hbar\tilde{\Omega}_p = 2\pi \times \lambda_p n_p \hbar X_2^{(l)} \hbar X_2^{(l)} E_{Lp} (E_{JO} E_{JX})^{-1} \\
c\hat{p}_0 &\sim \hat{\sigma}_x^{(1)} \hat{\sigma}_z^{(1)} c\hat{p}_0 = 2\pi \times \hbar X_1^{(1)} \hbar Z_1^{(1)} E_{JO}^{-1} \\
mc^2 &\sim \hbar\Omega = 2\pi \times Z_1^{(1)} n_m, \quad (p = x, y, z).
\end{aligned} \tag{4}$$

Then Hamiltonian  $H_{eff}$  obtained by the iteration is implemented by the diagonal transformation  $H_I = D^{-1}(\vartheta) H_{eff} D(\vartheta)$  with

$$D(\vartheta) = \begin{bmatrix} \cos(\vartheta/2) & -i \sin(\vartheta/2) \\ i \sin(\vartheta/2) & -\cos(\vartheta/2) \end{bmatrix},$$

one can obtain

$$H_I = mc^2 \hat{\sigma}_z^{(1)} I^{(2)} + \hat{\sigma}_x^{(1)} \hat{\sigma}^{(2)} cp + \hat{\sigma}_x^{(1)} \hat{\sigma}_z^{(1)} cp_0$$

The factors in the Hamiltonian are shown as

$$\begin{aligned}
\theta &= \arccos(z_0^{(l)} [(z_0^{(l)})^2 + (x_0^{(l)})^2]^{-1/2}) \\
\vartheta &= \arccos(Z_1^{(l)} [(Z_1^{(l)})^2 + (Z_3^{(l)} \omega_3)^2]^{-1/2}) \\
Z_i^{(l)} &= m_l z r_i^{(l)} \hat{\sigma}_z^{(l)}, \quad X_i^{(l)} = m_l x r_i^{(l)} \hat{\sigma}_x^{(l)} \\
\text{when } i &= 0, 1, 2, m_l = \mu_l; \quad i = 3, m_l = \nu_l; \quad l = 1, 2 \\
\mu_l &= 2\alpha_l E_J^{(l)} \cos(\pi f_1^{(l)}), \quad \nu_l = 2\beta_l / (1 + 4\beta_l) \\
z r_i^{(1)} &= x_i^{(1)} \cos\theta_1 - z_i^{(1)} \sin\theta_1, \quad x r_i^{(1)} = x_i^{(1)} \sin\theta_1 + z_i^{(1)} \cos\theta_1 \\
z r_i^{(2)} &= z_i^{(2)} \cos\theta_2 + x_i^{(2)} \sin\theta_2, \quad x r_i^{(2)} = z_i^{(2)} \sin\theta_2 - x_i^{(2)} \cos\theta_2 \\
z_0^{(l)} &= (\langle e_l | H_{q0}^{(l)} | e_l \rangle - \langle g_l | H_{q0}^{(l)} | g_l \rangle) / 2, \quad x_0^{(l)} = \langle e_l | H_{q0}^{(l)} | g_l \rangle \\
z_1^{(l)} &= (\langle e_l | \sin_l | e_l \rangle - \langle g_l | \sin_l | g_l \rangle) / 2, \quad x_1^{(l)} = \langle e_l | \sin_l | g_l \rangle \\
z_2^{(l)} &= (\langle e_l | \cos_l | e_l \rangle - \langle g_l | \cos_l | g_l \rangle) / 2, \quad x_2^{(l)} = \langle e_l | \cos_l | g_l \rangle \\
\sin_l &= \sin(2\varphi_a^{(l)} + 2\pi f_3^{(l)}), \quad \cos_l = \cos(2\varphi_a^{(l)} + 2\pi f_3^{(l)}) \\
z_3^{(l)} &= (\langle e_l | N_{al} | e_l \rangle - \langle g_l | N_{al} | g_l \rangle) \hbar / 2, \quad x_3^{(l)} = \langle e_l | \hbar N_{al} | g_l \rangle
\end{aligned}$$

The basis space  $\{|1D\rangle, |1U\rangle\}$  rotates to  $\{|10\rangle, |11\rangle\}$ . After implementing Lorentz transformation S on the hamiltonian

$$S = \begin{bmatrix} \cosh(az) & 0 & \sinh(az) & 0 \\ 0 & \cosh(az) & 0 & -\sinh(az) \\ -\sinh(az) & 0 & \cosh(az) & 0 \\ 0 & \sinh(az) & 0 & \cosh(az) \end{bmatrix} \tag{5}$$

with  $az = 0.5 \tanh^{-1}[-(cp_0/mc^2)[1 + (cp_0/mc^2)^2]^{-0.5}]$ , the standard form can be obtained

$$H_I = \begin{bmatrix} mc^2 & 0 & cp_z & c(p_x - ip_y) \\ 0 & mc^2 & c(p_x + ip_y) & -cp_z \\ cp_z & c(p_x - ip_y) & -mc^2 & 0 \\ c(p_x + ip_y) & -cp_z & 0 & -mc^2 \end{bmatrix} \tag{6}$$

with the basis space  $\{|10\rangle, |11\rangle\} \otimes \{|20\rangle, |21\rangle\} \otimes \{|n_x\rangle\} \otimes \{|n_y\rangle\} \otimes \{|n_z\rangle\}$

The zitterbewerg effect is observed according to the formula [1]

$$r(t) = r(0) + c^2 p H_I^{-1} t + \frac{c\alpha - c^2 p H_I^{-1}}{2iH_I} (e^{2iH_I t} - 1) \tag{7}$$

In 2+1D,  $p_z = 0$  in equation (6). Certainly, 1+1 Dirac equation is reduced equation (6),  $H_I = mc^2 \hat{\sigma}_z + cp_x \hat{\sigma}_x$  and 1+1D tremor is observed according to reduced formula (7).

Quantum states stored at the superconductivity quantum system have been dead accidentally from thermal noise [23] or  $1/f$  noise and geometric phase [24–26] prior to the decay naturally due to damping. Fig. 3 represents the decoherence time of each qubit in the system. Fig. 4 shows some other properties of the magnetic flux qubits, which related to decoherence. The flux qubits' scheme in Fig 1 is composite of schemes in reference [14–17]. The new flux qubit has a suitable shunt capacitor, a thinner barrier determined by the SQUID set at proper operating point, a larger ring inductor. These new features effectively reduces the dephasing of the charge noise, the magnetic noise, and effectively broadens the stable operating region of flux qubit [14–17]. Considering the AC component in the circling current, the coupling parameters of the flux qubit are fluctuating. When  $f_1^{(l)} \sim 0.3310$  or  $0.3555$ , the circling current is smaller,  $Z_1^{(l)}, X_1^{(l)}$  are smaller,  $Z_2^{(l)}, X_2^{(l)}$  are larger and stable. So, the operating point shift of flux qubit is smaller due to transition of adjacent flux qubit. For  $\sim MHz$  noise, the adiabatic condition is well met [24–26], the decoherence effects of the driving pulses are completely ignore. The coupling strength mapping to the kinetic energy is larger. For

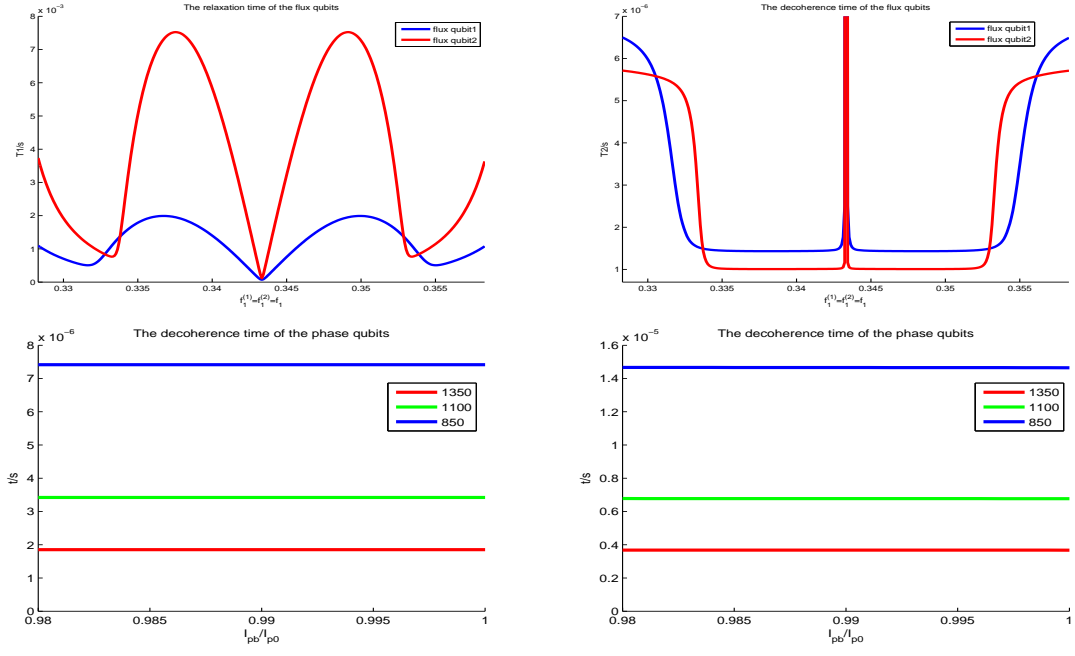


FIG. 3: the relaxation time and decoherence time of the qubits. The left graph is relaxation time and the right graph is decoherence time. The first depict the magnetic flux qubits, voltage bias capacitance  $C_g^{(l)} = 0$ , magnetic bias inductance  $m \sim 5pH$ . The second column depict phase qubits with  $E_{Jp}/\hbar = 850, 1100, 1350\text{GHz}$ , voltage bias capacitance satisfy  $C_{gp}/(C_{Jp} + C_{sh}) \sim 0$ , magnetic bias inductance  $m \sim 5pH$

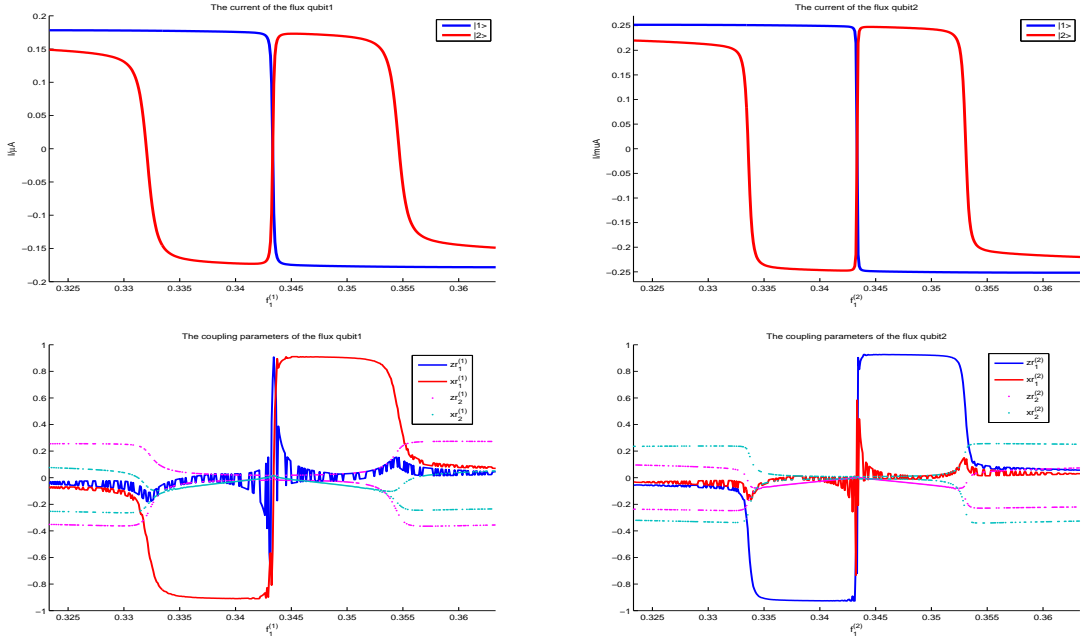


FIG. 4: The magnetic flux qubits' circling current and the coupling parameters ( $zr_i^{(l)}, xr_i^{(l)}, l = 1, 2; i = 1, 2$ ). Ground state,  $|0\rangle$ , excited state,  $|1\rangle$ . The coupling parameters satisfy  $Z_1^{(l)} = \mu_l zr_1^{(l)}, X_1^{(l)} = \mu_l xr_1^{(l)}, Z_2^{(l)} = \mu_l zr_2^{(l)}, X_2^{(l)} = \mu_l xr_2^{(l)}, \mu_l = 2\alpha_l E_J^{(l)} \cos(\pi f_1^{(l)})$

the phase qubits, a single crystal silicon shunt capacitor have released the relaxation time [27]. When operating point at  $I_{pb}/I_{p0} = 0.99$ ,  $\lambda_p$  is larger.

In the current low temperature conditions, about  $6mK$ , there is only a small influence of thermal fluctuation and photon noise [23, 29]. The thermal annealing has also enhanced dephasing time [31]. Nondestructive measurement reduces the damage from readout [32]. In our system, the ideal expected results can be obtained if the decoherence time can reach a microsecond. Resonance does not contribute to decoherence [33], then the shortest decoherence time among all the qubits under the strict conditions is closer to the lower bound of the decoherence time of the system.

In conclusion, we have designed experimentally feasible quantum simulators to simulate 3+1, 2+1, 1+1 Dirac equation.

We are grateful to H.Q. Lin, J.Q. You, Jiuqing Liang, Changjun Liao for fruitful discussions.

- 
- [1] L. Lamata, J. Len, T. Schütz, and E. Solano, Physical Review Letters **98**, 253005(2007).  
 [2] A. Bermudez, M. A. Martin-Delgado, and E. Solano, Physical Review A **76**, 041801(R)(2007).  
 [3] R. Gerritsma<sup>1,2</sup>, G. Kirchmair, F.Zähringer, E. Solano, R. Blatt and C. F. Roos, nature **463**, 68(2010).  
 [4] Xiangdong Zhang, Physical Review Letters **100**, 113903(2008).  
 [5] Xiangdong Zhang and Zhengyou Liu, Physical Review Letters **101**, 264303(2008).  
 [6] I. Chiorescu, P. Bertet, K. Semba, Y. Nakamura, C. J. P. M. Harmans, J. E. Mooij, Nature **431**, 159(2004).  
 [7] J. Q. You, Franco Nori, Nature **474**, 589(2011).  
 [8] A. Bermudez, M. A. Martin-Delgado, and E. Solano, Physical Review Letters **99**, 123602(2007).  
 [9] Jzsef Cserti and Gyula Dvid, Physical Review B **74**, 172305(2006).  
 [10] Yu-Xi Liu, J. Q. You, L. F. Wei, C. P. Sun, and Franco Nori, Physical Review Letters **95**, 087001(2005).  
 [11] Yuriy Makhlin, Gerd Schon, Alexander Shnirman, Reviews of Modern Physics **73**, 357(2001).  
 [12] Iulia Buluta, Franco Nori, Science **326**, 108(2009). I. M. Georgescu, S. Ashhab, Franco Nori, Reviews of Modern Physics **86**, 153.  
 [13] Abhinav Kandala, Antonio Mezzacapo, Kristan Temme, Maika Takita, Markus Brink, Jerry M. Chow, Jay M. Gambetta, Nature **549**, 242(2017).  
 [14] J. E. Mooij, T. P. Orlando, L. Levitov, Lin Tian, Caspar H. van der Wal, Seth Lloyd, Science **285**, 1036(1999).  
 [15] T. P. Orlando, J. E. Mooij, Lin Tian, Caspar H. van der Wal, L. S. Levitov, Seth Lloyd, J. J. Mazo, Physical Review B **60**, 15398(1999).  
 [16] A. O. Niskanen, K. Harrabi, F. Yoshihara, Y. Nakamura, and J. S. Tsai, Physical Review B **74**, 220503(R)(2006).  
 [17] J. Q. You, Xuedong Hu, Ashhab, and Franco Nori, Physical Review B **75**, 140515(R)(2007).  
 [18] Xiao-Ling He, J. Q. You, Yu-xi Liu, L. F. Wei and Franco Nori, Physical Review B **76**, 024517(2007).  
 [19] Yu-xi Liu, L. F. Wei, J. S. Tsai, and Franco Nori, Physical Review Letters **96**, 067003(2006).  
 [20] J. Q. You, Y. Nakamura, and Franco Nori, Physical Review B **71**, 024532(2005).  
 [21] Kaushik Mitra, F. W. Strauch, C. J. Lobb, J. R. Anderson, and F. C. Wellstood, Physical Review B **77**, 214512(2008).  
 [22] Alec Maassen van den Brink, Physical Review B **71**, 064503(2005).  
 [23] Samuele Spilla, Fabian Hassler and Janine Splettstoesser, New Journal of Physics **16**, 045020(2014).  
 [24] E. Paladino, Y. M. Galperin, G. Falci, B. L. Altshuler, Reviews of Modern Physics **86**, 361(2014).  
 [25] S. Berger, M. Pechal, P. Kurpiers, A.A. Abdumalikov, C. Eichler, w, J.A. Mlynek, A. Shnirman, Yuval Gefen, A. Wallraff, S. Philipp, Nature Communications **6**, 8757  
 [26] P.J.Leek, J. M. Fink, A. Blais, R. Bianchetti, M.Göppel, J.M.Gambetta, D.I.Schuster, L.Frunzio, R.J.Schoelkopf, A.Wallraff Science **318**, 1889(2007).  
 [27] U. Patel, Y. Gao, D. Hover, G. J. Ribeill, S. Sendelbach, and R. McDermott, Applied Physics Letters **102**, 012602(2013).  
 [28] J. Q. You, J. S. Tsai, and Franco Nori, Physical Review B **73**, 014510(2006).  
 [29] P. Bertet, I. Chiorescu, G. Burkard, K. Semba, C. J. P. M. Harmans, D. P. DiVincenzo, and J. E. Mooij, Physical Review Letters **95**, 257002(2005).  
 [30] Jonas Bylander, Simon Gustavsson, Fei Yan, Fumiki Yoshihara, Khalil Harrabi, George Fitch, David G. Cory Yasunobu Nakamura, Jaw-Shen Tsai and William D. Oliver, Nature Physics **7**, 565(2011).  
 [31] J. K. Julin, P. J. Koppinen, and I. J. Maasilta, Applied Physics Letters **97**, 152501(2010);  
 [32] A. Lupascu, E. F. C. Driessen, L. Roschier, C. J. P. M. Harmans, and J. E. Mooij, Physical Review Letters **96**, 127003(2006).  
 [33] Zhongyuan Zhou, Shih-I Chu and Siyuan Han, J. Phys. B: At. Mol. Opt. Phys. **41**, 045506(2008).

Appendix: Details of the iterative calculations

Part A: Quantization of the flux qubit

Part B: Quantization of the phase qubit

Part C: calculation of decoherence time

Part D: Details of the iteration calculation



From the view of quantum theory, we calculate the coupling between three qubits driven resonantly by the driving pulses and prove the inductance of the Josephson junction is  $\Phi_0^2/(4\pi^2 E_J)$ , which is consistent with the classic conclusion. To be simplified,  $\hat{a}^-$  represents annihilation operator, Einstein summation symbol is applied. "  $\pm$  " is the same in the following cases:  $\hat{\sigma}_\pm^{(2)}$  and  $\pm 2\varepsilon_2$ ;  $\hat{a}_x^\pm$  and  $\pm\omega_x$ ;  $\pm\omega_i^{(1)}$  and  $\pm\phi_i^{(1)}$ ;  $\pm\omega_i^{(2)}$  and  $\pm\phi_i^{(2)}$ ; The left  $\hat{a}_P^\pm$  in the  $\hat{a}_P^\pm\hat{a}_P^\pm$  and the left  $\pm\omega_P$  in the  $\pm\omega_P \pm\omega_P$  in the exponential expression and the leftmost  $\pm\omega_P$  in the denominator; The right  $\hat{a}_P^\pm$  in the  $\hat{a}_P^\pm\hat{a}_P^\pm$  and the right  $\pm\omega_P$  in the  $\pm\omega_P \pm\omega_P$  in the exponential expression and the other  $\pm\omega_P$  in the denominator.

Part A: Quantization of the flux qubit [17–22]

When ring inductance  $L_r \rightarrow 0$ , the Hamiltonian of the system is shown as[22]

$$\begin{aligned} H &= \sum_{i=1}^4 [(\Phi_0/2\pi)^2 C_i \dot{\varphi}_i^2/2 + E_{Ji}(1 - \cos \varphi_i)] + L_r I^2/2 \\ &= 1/2 C [ Q_1 \quad Q_2 ] \begin{bmatrix} 1+\beta & \beta \\ \beta & 1+\beta \end{bmatrix} \begin{bmatrix} Q_1 \\ Q_2 \end{bmatrix} - E_J \cos \varphi_1 - E_J \cos \varphi_2 - 2\alpha E_J \cos(\pi f_2) \cos(\varphi_1 + \varphi_2 + 2\pi f_1 + \pi f_2) \\ &= [ Q_1 \quad Q_2 ] \begin{bmatrix} \frac{1+\beta}{2(1+2\beta)C} & \frac{-\beta}{2(1+2\beta)C} \\ \frac{-\beta}{2(1+2\beta)C} & \frac{1+\beta}{2(1+2\beta)C} \end{bmatrix} \begin{bmatrix} Q_1 \\ Q_2 \end{bmatrix} - E_J \cos \varphi_1 - E_J \cos \varphi_2 - 2\alpha E_J \cos(\pi f_2) \cos(\varphi_1 + \varphi_2 + 2\pi f_1 + \pi f_2) \\ &= \frac{(1+\beta)Q_1^2}{2(1+2\beta)C} + \frac{(1+\beta)Q_2^2}{2(1+2\beta)C} - \frac{\beta Q_1 Q_2}{(1+2\beta)C} - E_J \cos \varphi_1 - E_J \cos \varphi_2 - 2\alpha E_J \cos(\pi f_2) \cos(\varphi_1 + \varphi_2 + 2\pi f_1 + \pi f_2) \end{aligned}$$

the first derivative of the phase  $\varphi_1$  is shown as

$$\dot{\varphi}_1 = \frac{i}{\hbar} [H, \varphi_1] = \frac{i}{\hbar} \frac{2e}{i} \frac{(1+\beta)}{(1+2\beta)C} \frac{2e}{i} \frac{\partial}{\partial \varphi_1} + \frac{i}{\hbar} \frac{2e}{i} \frac{-\beta}{(1+2\beta)C} Q_2 = \frac{2\pi}{\Phi_0} \frac{(1+\beta)}{(1+2\beta)C} \frac{\partial}{\partial \varphi_1} + \frac{2\pi}{\Phi_0} \frac{-\beta}{(1+2\beta)C} Q_2$$

the second derivative of the phase  $\varphi_1$  is shown as

$$\ddot{\varphi}_1 = \frac{i}{\hbar} [H, \dot{\varphi}_1] = - \left( \frac{2\pi}{\Phi_0} \right)^2 \frac{1}{C} E_J \left[ \frac{1+\beta}{1+2\beta} \sin \varphi_1 + \frac{-\beta}{1+2\beta} \sin \varphi_2 + \frac{2\alpha \cos(\pi f_2)}{1+2\beta} \sin(\varphi_1 + \varphi_2 + 2\pi f) \right]$$

the current of junction1 in the flux qubit

$$I_0 = I_{c1} \sin \varphi_1 + C_1 \frac{\Phi_0}{2\pi} \ddot{\varphi}_1 = \frac{2\pi}{\Phi_0} \frac{\beta}{1+2\beta} E_J [\sin \varphi_1 + \sin \varphi_2 - 2(\alpha/\beta) \cos(\pi f_2) \sin(\varphi_1 + \varphi_2 + 2\pi f)]$$

the Hamiltonian of the flux qubit with ring inductance  $L_r$  by driving pulses represents as

$$\begin{aligned} H_q^{(l)} &= 2E_{C_a}^{(l)} N_{al}^2 + 2E_{C_s}^{(l)} N_{sl}^2 + 2E_J^{(l)} + 2\alpha_l E_J^{(l)} \\ &\quad - 2E_J^{(l)} \cos \varphi_a^{(l)} \cos \varphi_s^{(l)} - 2\alpha_l E_J^{(l)} \cos(\pi f_2^{(l)}) \cos(2\varphi_s^{(l)} + 2\pi f_3^{(l)}) \\ &\quad + 2\alpha_l E_J^{(l)} \cos(\pi f_2^{(l)}) \sin(2\varphi_s^{(l)} + 2\pi f_3^{(l)}) [\varphi_r^{(l)} + \sum_{i=1}^3 \Phi_i^{(l)}] \\ &\quad + \alpha_l E_J^{(l)} \cos(\pi f_2^{(l)}) \cos(2\varphi_s^{(l)} + 2\pi f_3^{(l)}) [\varphi_r^{(l)} + \sum_{i=1}^3 \Phi_i^{(l)}]^2 \\ &\quad + [2\beta_1/(1+4\beta_l)] \hbar N_s^{(l)} \sum_{i=1}^3 \dot{\Phi}_i^{(l)} + \frac{1}{2} L [I^{(l)}]^2 \end{aligned}$$

When ring inductance  $L_r \neq 0$ , the Hamiltonian of the system is shown as

$$H = \sum_{i=1}^4 [(\Phi_0/2\pi)^2 C_i \dot{\varphi}_i^2/2 + E_{Ji}(1 - \cos \varphi_i)] + \frac{1}{2} L (2\pi E_{J1}/\Phi_0)^2 \sin^2 \varphi_1$$

The circling current is approximated as

$$I_0 = \frac{2\pi}{\Phi_0} \frac{\beta}{1+2\beta} E_J [\sin \varphi_1 + \sin \varphi_2 - 2(\alpha/\beta) \cos(\pi f_2) \sin(\varphi_1 + \varphi_2 + 2\pi f) + l \sin \varphi_1 \cos \varphi_1]$$

Here,  $l = L_r/L_J$ ,  $L_r$  ring inductance,  $L_J$  junction inductance.

Numerical solution shows that there is little difference in the two cases with  $l = 0.17$ ;  $l = 0.23$ .

The Hamiltonian of the bare flux qubit biased static magnetic fluxes represents as[22]

$$H_{q_0}^{(l)} = 2E_{C_a}^{(l)} N_{al}^2 + 2E_{C_s}^{(l)} N_{sl}^2 - 2E_J^{(l)} \cos \varphi_s^{(l)} \cos \varphi_a^{(l)} - 2\alpha_l E_J^{(l)} \cos(\pi f_2^{(l)}) \cos(2\varphi_s^{(l)} + 2\pi f_3^{(l)}) - L_r^{(l)} (I_0^{(l)})^2/2$$



corresponding circling current represents as

$$I_0^{(l)} = [\beta_l/(1 + 2\beta_l)](2\pi/\Phi_0)E_J^{(l)} [2 \sin \varphi_s^{(l)} \cos \varphi_a^{(l)} - (2\alpha_l/\beta_l) \cos(\pi f_2^{(l)}) \sin(2\varphi_s^{(l)} + 2\pi f_3^{(l)})]$$

$$H_{q0}^{(l)} = z_0^{(l)} \hat{\sigma}_z^{(l)} + x_0^{(l)} \hat{\sigma}_x^{(l)}$$

the Hamiltonian of  $H_q^{(l)}$  is transformed into

$$H_D^{(l)} = D_l^T(\theta_l/2) H D_l(\theta_l/2), \quad \theta_l = \arccos(z_0^{(l)} [(z_0^{(l)})^2 + (x_0^{(l)})^2]^{1/2}),$$

$$D_1(\theta_1) = \begin{bmatrix} \cos(\pi/4 + \theta_1/2) & \sin(\pi/4 + \theta_1/2) \\ \sin(\pi/4 + \theta_1/2) & -\cos(\pi/4 + \theta_1/2) \end{bmatrix}, \quad D_2(\theta_2) = \begin{bmatrix} \cos(\theta_2/2) & \sin(\theta_2/2) \\ \sin(\theta_2/2) & \cos(\theta_2/2) \end{bmatrix}$$

$H_{q0}^{(1)}, H_{q0}^{(2)}$  are transformed into

$$H_{D0}^{(1)} = X_0^{(1)} \hat{\sigma}_x^{(1)}, \quad H_{D0}^{(2)} = Z_0^{(2)} \hat{\sigma}_z^{(2)}$$

Part B: the quantization of the phase qubit:

Define the phase

$$\varphi_{p1} = \varphi_p - \varphi_{p0},$$

$$\gamma_{P1} = \gamma_P - \gamma_{P0},$$

bias current

$$\sin \varphi_{p0} = I_{pb}/I_{p0},$$

the phase relationship:

$$\varphi_{p0} - \gamma_{P0} + 2\pi\Phi_p/\Phi_0 = 0,$$

the effective coupling energy of the inductance  $L_{rp}$

$$E_{rp} = (\Phi_0/2\pi)^2/L_{rp},$$

The Hamiltonian of the phase qubit  $p$

$$\begin{aligned} H_p &= 4E_{cp}N_p^2 - E_{Jp}(\cos \varphi_p + I_{pb}\varphi_p/I_{p0}) + \frac{1}{2}E_{rp}(\varphi_p - \varphi_{p0})^2 \\ &= 4E_{cp}N_p^2 - E_{Jp}[\cos \varphi_{p1} \cos \varphi_{p0} - \sin \varphi_{p1} \sin \varphi_{p0} + \varphi_{p1} \sin \varphi_{p0} + \varphi_{p0} \sin \varphi_{p1}] + \frac{1}{2}E_{rp}(\varphi_p - \varphi_{p0})^2 \\ &= 4E_{cp}N_p^2 - E_{Jp}[\cos \varphi_{p1} \cos \varphi_{p0} - \varphi_{p1} \sin \varphi_{p0} + \varphi_{p1} \sin \varphi_{p0} + \varphi_{p0} \sin \varphi_{p1}] + \frac{1}{2}E_{rp}(\varphi_p - \varphi_{p0})^2 \\ &= 4E_{cp}N_p^2 - E_{Jp}[\cos \varphi_{p1} \cos \varphi_{p0} + \varphi_{p0} \sin \varphi_{p1}] + \frac{1}{2}E_{rp}(\varphi_p - \varphi_{p0})^2 \\ &= 4E_{cp}N_{p1}^2 + \frac{1}{2}E_{Jp} \cos \varphi_{p0} \varphi_{p1}^2 + \frac{1}{2}E_{rp}(\varphi_p - \varphi_{p0})^2 \\ &= 4E_{cp}N_{p1}^2 + \frac{1}{2}(E_{Jp} \cos \varphi_{p0} + E_{rp})\varphi_{p1}^2 \end{aligned}$$

In the population representation:

$$\varphi_{p1} = \lambda_p(\hat{a}_p^+ + \hat{a}_p), \quad N_p = i(\hat{a}_p^+ - \hat{a}_p)/2\lambda_p,$$

The boson operator

$$\hat{a}_p^+ = \varphi_{p1}/(2\lambda_p) - i\lambda_p N_p, \quad \hat{a}_p = \varphi_{p1}/(2\lambda_p) + i\lambda_p N_p$$

$$\lambda_p = [2E_{Cp}/(E_{Jp} \cos \varphi_{p0} + E_{rp})]^{1/4}, \quad \hbar\omega_p = [8E_{Cp}(E_{Jp} \cos \varphi_{p0} + E_{rp})]^{1/2}$$

the Hamiltonian is secondary quantized to

$$H_p = \hbar\omega_p(\hat{a}_p^+ \hat{a}_p + 1/2)$$

Total Hamiltonian is described as

$$\begin{aligned} H_I = & \hbar X_0^{(1)} \hat{\sigma}_x^{(1)} + \hbar X_0^{(2)} \hat{\sigma}_z^{(2)} + \sum_{P=C} \hbar\omega_P \hat{a}_P^+ \hat{a}_P + \sum_{p=c} \hbar\omega_p \hat{a}_p^+ \hat{a}_p + \hbar\omega_O \hat{a}_O^+ \hat{a}_O \\ & + (\hbar Z_1^{(l)} \hat{\sigma}_z^{(l)} + \hbar X_1^{(l)} \hat{\sigma}_x^{(l)}) [((-1)^l \lambda_O \hat{a}_O^+ + \sum_{P_l=C_l} \lambda_{P_l} \hat{a}_{P_l}^+ + \sum_{r=R_l} \frac{1}{2} n_r^{(l)} e^{\omega_r^{(l)} it + i\phi_r^{(l)}}) + H.C] \\ & + (\hbar Z_2^{(l)} \hat{\sigma}_z^{(l)} + \hbar X_2^{(l)} \hat{\sigma}_x^{(l)}) [((-1)^l \lambda_O \hat{a}_O^+ + \sum_{P_l=C_l} \lambda_{P_l} \hat{a}_{P_l}^+ + \sum_{r=R_l} \frac{1}{2} n_r^{(l)} e^{\omega_r^{(l)} it + i\phi_r^{(l)}}) + H.C]^2 \\ & + (\hbar Z_3^{(l)} \hat{\sigma}_z^{(l)} + \hbar X_3^{(l)} \hat{\sigma}_x^{(l)}) \sum_{r=R_l} \frac{1}{2} n_r^{(l)} \omega_r^{(l)} (e^{\omega_r^{(l)} it + i(\phi_r^{(l)} - \pi/2)} + H.C) \\ & + E_{Lp} [\sum_{pP} (\lambda_p \hat{a}_p^+ - \lambda_P \hat{a}_P^+) + H.C]^2 \end{aligned}$$

$$\begin{aligned} 3 + 1D : & C = X, Y, Z; c = x, y, z; R_l = 3; l = 1 : C_l = X, Z; p = x, z; l = 2 : C_l = Y; p = y; \\ & pP : p = x \& P = X; p = y \& P = Y; p = z \& P = Z; \\ 2 + 1D : & C = X, Y, T; c = x, y, z; l = 1 : C_l = X; p = x; R_l = 3; l = 2 : C_l = Y; p = y; R_l = 2 \\ & pP : p = x \& P = X; p = y \& P = Y; \\ 1 + 1D : & C = X; c = x; R_l = 2; \lambda_O = 0; l = 1 : C_l = X; pP : p = x \& P = X; \end{aligned}$$

the factors in the Hamiltonian are shown as

$$\begin{aligned} Z_i^{(l)} &= m_l z r_i^{(l)} \hat{\sigma}_z^{(l)}, \quad X_i^{(l)} = m_l x r_i^{(l)} \hat{\sigma}_x^{(l)} \\ \text{when } i &= 0, 1, 2, \quad m_l = \mu_l; \quad i = 3, \quad m_l = \nu_l; \quad l = 1, 2 \\ \mu_l &= 2\alpha_l E_j^{(l)} \cos(\pi f_1^{(l)}), \quad \nu_l = 2\beta_l / (1 + 4\beta_l) \\ \theta_l &= \arccos(z_0^{(l)} [(z_0^{(l)})^2 + (x_0^{(l)})^2]^{-1/2}) \\ z r_i^{(1)} &= x_i^{(1)} \cos \theta_1 - z_i^{(1)} \sin \theta_1, \quad x r_i^{(1)} = x_i^{(1)} \sin \theta_1 + z_i^{(1)} \cos \theta_1 \\ z r_i^{(2)} &= z_i^{(2)} \cos \theta_2 + x_i^{(2)} \sin \theta_2, \quad x r_i^{(2)} = z_i^{(2)} \sin \theta_2 - x_i^{(2)} \cos \theta_2 \\ z_0^{(l)} &= (\langle e_l | H_{q0}^{(l)} | e_l \rangle - \langle g_l | H_{q0}^{(l)} | g_l \rangle) / 2, \quad x_0^{(l)} = \langle e_l | H_{q0}^{(l)} | g_l \rangle, \\ z_1^{(l)} &= (\langle e_l | \sin_l | e_l \rangle - \langle g_l | \sin_l | g_l \rangle) / 2, \quad x_1^{(l)} = \langle e_l | \sin_l | g_l \rangle \\ z_2^{(l)} &= (\langle e_l | \cos_l | e_l \rangle - \langle g_l | \cos_l | g_l \rangle) / 2, \quad x_2^{(l)} = \langle e_l | \cos_l | g_l \rangle \\ \sin_l &= \sin(2\varphi_a^{(l)} + 2\pi f_3^{(l)}), \quad \cos_l = \cos(2\varphi_a^{(l)} + 2\pi f_3^{(l)}) \\ z_3^{(l)} &= (\langle e_l | P_{al} | e_l \rangle - \langle g_l | P_{al} | g_l \rangle) / 2, \quad x_3^{(l)} = \langle e_l | P_{al} | g_l \rangle \end{aligned}$$

Part C: calculation of decoherence time

The decoherence time is calculated as

$$\begin{aligned} \Gamma_1 &= \sum_i |B_i|^2 S_i(\omega_{10}) = \frac{(Q_i)^2}{\hbar^2} \left( \frac{C_g}{C} \right)^2 \hbar (2\pi\omega_{10}) \text{Re}[Z(\omega_{10})] + \frac{(I)^2}{\hbar^2} M^2 \hbar (2\pi\omega_{10}) \text{Re}[Y(\omega_{10})] \\ \Gamma_\varphi &= \sum_i |A_i| [\alpha_i \ln(\omega_t/\omega_c)]^{0.5} \\ \Gamma_2 &= \Gamma_1/2 + \Gamma_\varphi \\ T_1 &= 1/\Gamma_1 \\ T_2 &= 1/\Gamma_2 \end{aligned}$$

Here,  $Q_i$  is charge in junction capacitor,  $I$  is the circling current,  $C_g$  is gate capacitance,  $C$  is junction capacitance,  $M$  is bias inductance. In our scheme, no voltage source is applied, so  $C_g = 0$ .

For the frequency of driving field  $\omega_i^{(l)} > 5GHz$ , the geometric dephasing is caused low frequency noise in the driving field rather than the driving field itself [24–26]. The detuning  $\Delta_i^{(1)} = 2X_0^{(1)} - \omega_i^{(1)} > 5GHz$ ,  $\Delta_i^{(2)} = 2Z_0^{(1)} - \omega_i^{(2)} > 5GHz$ , the coupling strength between the flux qubit and driving field  $\hbar\Omega_i^{(1)} = \hbar[(Z_1^{(1)})^2 + (Z_3^{(1)}\omega_3)^2]^{1/2} n_i^{(1)}$ ,  $\hbar\Omega_i^{(2)} = \hbar[(X_1^{(2)})^2 + (X_3^{(2)}\omega_3)^2]^{1/2} n_i^{(2)}/2$ . According to Fig4,  $\Omega_i^{(l)}/[(\Delta_i^{(l)})^2 + (\Omega_i^{(l)})^2]^{1/2} < 0.1$ . For  $\sim MHz$  noise,

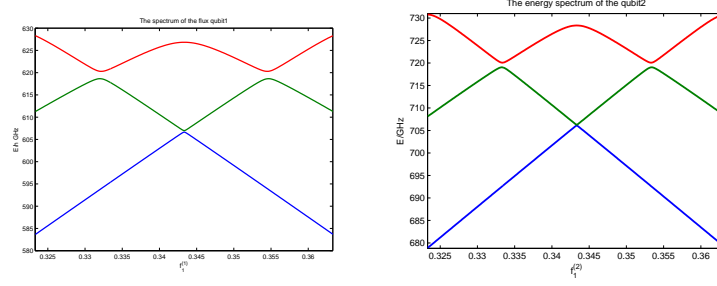


FIG. 5: The magnetic flux qubits' energy spectrum

the adiabatic condition is well met [26], which means the geometric phase is very small but exists. Inspired by spin echo [26], the dephasing effects of driving fields with opposite phase are counteracted each other. The dephasing effects are also counteracted by low frequency fields induced [24].

#### Part D: Details of the iteration calculation

In 3+1D, the first order approximation is resonant coupling term between the flux qubit1 and weak time-dependent magnetic fluxes, corresponding to the rest mass of the particles. It is shown as  $H_{I1} = \hbar Z_1^{(1)} n_3^{(1)} \sigma_z^{(1)} + \hbar \omega_3 Z_3^{(1)} n_3^{(1)} \sigma_y^{(1)}$ . The second order approximation has been considered because it is related to self-coupling of qubit. The third order approximation is the resonant coupling term between two flux qubits, one phase qubit and weak time-dependent magnetic fluxes, corresponding to the momentum-spin coupling of the particles. It can be obtained by iteration of  $H_{I3} = \sum I_j \int_0^{t_1} I_k dt_2 \int_0^{t_2} I_m dt_3$ , where  $j, k, m = 1, 2, 3$  and  $j \neq k \neq m$  [17–22]. All calculations satisfy the conditions of the frequencies:

$$\begin{aligned}
&+2X_0^{(1)} - \omega_3^{(1)} = 0, \quad \phi_3^{(1)} = 0, \quad n_3^{(1)} = n_m \\
&+\omega_z - \omega_3^{(2)} = 0, \quad \phi_3^{(2)} = -\pi/2, \quad n_3^{(2)} = n_z \\
&+2Z_0^{(2)} + \omega_y - \omega_1^{(1)} = 0, \quad \phi_1^{(1)} = 0, \quad n_1^{(1)} = n_y \\
&+2Z_0^{(2)} - \omega_y - \omega_2^{(1)} = 0, \quad \phi_2^{(1)} = \pi, \quad n_2^{(1)} = n_y \\
&+2Z_0^{(2)} + \omega_x - \omega_1^{(2)} = 0, \quad \phi_1^{(2)} = -\pi/2, \quad n_1^{(2)} = n_x \\
&+2Z_0^{(2)} - \omega_x - \omega_2^{(2)} = 0, \quad \phi_2^{(2)} = +\pi/2, \quad n_2^{(2)} = n_x \\
&\omega_O \gg \omega_X \neq \omega_Y \neq \omega_Z \gg 2X_0^{(1)}, 2Z_0^{(2)}, \omega_i^{(l)}
\end{aligned}$$

The shared junctions' parameters are shown as:  $\lambda_O = (2E_{CO}/E_{JO})^{1/4}$ ,  $\hbar\omega_O = (8E_{JO}E_{CO})^{1/2}$ ,  $E_{CO} = e^2/(2C_O)$ ,  $\lambda_P = [2E_{CP}/(E_{JP} \cos \gamma_{P0} + E_{LP})]^{1/4} \approx [2E_{CP}/E_{JP}]^{1/4}$ ,  $\hbar\omega_P = [8(E_{JP} \cos \gamma_{P0} + E_{LP})E_{CP}]^{1/2} \approx [8E_{JP}E_{CP}]^{1/2}$ ,  $E_{CP} = e^2/(2C_P)$

The coupling between momentum and spin in the x direction can be obtained by the iteration where

$$\begin{aligned}
I_1 &= -\hbar X_2^{(1)} \hat{\sigma}_x^{(1)} (\lambda_X \hat{a}_X^\dagger e^{+\omega_X it} + H.C.) (\lambda_O \hat{a}_O^\dagger e^{+\omega_O it} + H.C.), \\
I_2 &= +\hbar X_2^{(2)} (\hat{\sigma}_+^{(2)} e^{+2\varepsilon_2 it} + H.C.) (\lambda_O \hat{a}_O^\dagger e^{+\omega_O it} + H.C.) (\frac{1}{2} n_i^{(2)} e^{+i(\omega_i^{(2)} t + \phi_i^{(2)})} + H.C.), \\
I_3 &= -E_L (\lambda_x \hat{a}_x^\dagger e^{+\omega_x it} + H.C.) (\lambda_X \hat{a}_X^\dagger e^{+\omega_X it} + H.C.).
\end{aligned}$$

$$\begin{aligned}
&I_1 \int_0^t I_2 dt \int_0^t I_3 dt \\
&= -\hbar X_2^{(1)} \hat{\sigma}_x^{(1)} \lambda_X \hat{a}_X^\dagger e^{+\omega_X it} \lambda_O \hat{a}_O^\dagger e^{+\omega_O it} \\
&\times \int_0^t \hbar X_2^{(2)} \hat{\sigma}_\pm^{(2)} e^{\pm 2\varepsilon_2 it} \lambda_O \hat{a}_O^\dagger e^{+\omega_O it} \frac{1}{2} n_i^{(2)} e^{\pm \omega_i^{(2)} it} e^{\pm \phi_i^{(2)} i} dt_1 \\
&\times \int_0^{t_1} [-E_L \lambda_x \lambda_X \hat{a}_x^\dagger e^{+\omega_x it} + H.C.] dt_2 \\
&= \hbar X_2^{(1)} \hbar X_2^{(2)} E_L \lambda_X \lambda_X \lambda_O \lambda_O \lambda_x \frac{1}{2} n_i^{(2)} \hat{a}_\pm^\dagger \hat{a}_X^\dagger \hat{a}_O^\dagger \hat{\sigma}_\pm^{(1)} \hat{\sigma}_\pm^{(2)} \hat{a}_x^\dagger e^{\pm \phi_i^{(2)} i} \frac{e^{(\pm \omega_X \pm \omega_X \pm \omega_O \pm \omega_O \pm 2\varepsilon_2 \pm \omega_i^{(2)} \pm \omega_x) it}}{(\pm \omega_O \pm \omega_X) i \pm \omega_X i} \\
&\approx \hbar X_2^{(1)} \hbar X_2^{(2)} E_L \lambda_X \lambda_X \lambda_O \lambda_O \lambda_x \frac{1}{2} n_i^{(2)} \hat{a}_\pm^\dagger \hat{a}_X^\dagger \hat{a}_O^\dagger \hat{\sigma}_\pm^{(1)} \hat{\sigma}_\pm^{(2)} \hat{a}_x^\dagger e^{\pm \phi_i^{(2)} i} \frac{e^{(\pm \omega_X \pm \omega_X \pm \omega_O \pm \omega_O \pm 2\varepsilon_2 \pm \omega_i^{(2)} \pm \omega_x) it}}{(\pm \omega_O) i (\pm \omega_X) i} \\
&= \hbar X_2^{(1)} \hbar X_2^{(2)} E_L \lambda_X \lambda_X \lambda_O \lambda_O \lambda_x \frac{1}{2} n_i^{(2)} \times \\
&\left( \begin{aligned}
&+\hat{a}_X^- \hat{a}_X^+ \hat{a}_O^- \hat{a}_O^+ \hat{\sigma}_x^{(1)} \hat{\sigma}_\pm^{(2)} \hat{a}_\pm^\dagger e^{\pm \phi_i^{(2)} i} \frac{e^{(\pm 2\varepsilon_2 \pm \omega_i^{(2)} \pm \omega_x) it}}{(+\omega_O) i (+\omega_X) i} + \hat{a}_X^- \hat{a}_X^+ \hat{a}_O^- \hat{a}_O^+ \hat{\sigma}_x^{(1)} \hat{\sigma}_\pm^{(2)} \hat{a}_\pm^\dagger e^{\pm \phi_i^{(2)} i} \frac{e^{(\pm 2\varepsilon_2 \pm \omega_i^{(2)} \pm \omega_x) it}}{(-\omega_O) i (+\omega_X) i} \\
&+\hat{a}_X^+ \hat{a}_X^- \hat{a}_O^- \hat{a}_O^+ \hat{\sigma}_x^{(1)} \hat{\sigma}_\pm^{(2)} \hat{a}_\pm^\dagger e^{\pm \phi_i^{(2)} i} \frac{e^{(\pm 2\varepsilon_2 \pm \omega_i^{(2)} \pm \omega_x) it}}{(+\omega_O) i (-\omega_X) i} + \hat{a}_X^+ \hat{a}_X^- \hat{a}_O^- \hat{a}_O^+ \hat{\sigma}_x^{(1)} \hat{\sigma}_\pm^{(2)} \hat{a}_\pm^\dagger e^{\pm \phi_i^{(2)} i} \frac{e^{(\pm 2\varepsilon_2 \pm \omega_i^{(2)} \pm \omega_x) it}}{(-\omega_O) i (-\omega_X) i}
\end{aligned} \right) \\
&= \hbar X_2^{(1)} \hbar X_2^{(2)} E_L \frac{\lambda_X \lambda_X \lambda_O \lambda_O}{\omega_O i \omega_X i} \lambda_x \frac{1}{2} n_i^{(2)} \hat{\sigma}_x^{(1)} \hat{\sigma}_\pm^{(2)} \hat{a}_\pm^\dagger e^{\pm \phi_i^{(2)} i} e^{(\pm 2\varepsilon_2 \pm \omega_i^{(2)} \pm \omega_x) it} \\
&= \hbar X_2^{(1)} \hbar X_2^{(2)} E_L (4E_{JX} E_{JO})^{-1} \lambda_x \frac{1}{2} n_i^{(2)} \hat{\sigma}_x^{(1)} \hat{\sigma}_\pm^{(2)} \hat{a}_\pm^\dagger e^{\pm \phi_i^{(2)} i} e^{(\pm 2\varepsilon_2 \pm \omega_i^{(2)} \pm \omega_x) it}
\end{aligned}$$



$$\begin{aligned}
& I_3 \int_0^t I_2 dt \int_0^t I_1 dt = \\
& = -E_L \lambda_x \lambda_X \hat{a}_x^\pm \hat{a}_X^\pm e^{(\pm\omega_x \pm \omega_X)it} \\
& \times \int_0^t X_2^{(2)} \hat{\sigma}_\pm^{(2)} e^{\pm 2\varepsilon_2 it} \lambda_O \hat{a}_O^\pm e^{\pm \omega_O it} \frac{1}{2} n_i^{(2)} e^{\pm \omega_i^{(2)} it} e^{\pm \phi_i^{(2)} i} dt_1 \\
& \times \int_0^{t_1} [-X_2^{(1)} \hat{\sigma}_x^{(1)} \lambda_X \hat{a}_X^\pm e^{\pm \omega_X it} \lambda_O \hat{a}_O^\pm e^{\pm \omega_O it}] dt_2 \\
& = \hbar X_2^{(2)} \hbar X_2^{(1)} E_L \lambda_X \lambda_X \lambda_O \lambda_O \lambda_x \frac{1}{2} n_i^{(2)} \hat{a}_X^\pm \hat{a}_X^\pm \hat{a}_O^\pm \hat{a}_O^\pm \hat{\sigma}_x^{(1)} \hat{\sigma}_\pm^{(2)} \hat{a}_x^\pm e^{\pm \phi_i^{(2)} i} \frac{e^{(\pm\omega_X \pm \omega_X \pm \omega_O \pm \omega_O \pm \omega_x \pm 2\varepsilon_2 \pm \omega_i^{(2)})it_2}}{(\pm\omega_O \pm \omega_X \pm \omega_O)i(\pm\omega_X \pm \omega_O)i} \\
& \approx \hbar X_2^{(2)} \hbar X_2^{(1)} E_L \lambda_X \lambda_X \lambda_O \lambda_O \lambda_x \frac{1}{2} n_i^{(2)} \hat{a}_X^\pm \hat{a}_X^\pm \hat{a}_O^\pm \hat{a}_O^\pm \hat{\sigma}_x^{(1)} \hat{\sigma}_\pm^{(2)} \hat{a}_x^\pm e^{\pm \phi_i^{(2)} i} \frac{e^{(\pm\omega_X \pm \omega_X \pm \omega_T \pm \omega_T \pm \omega_x \pm 2\varepsilon_2 \pm \omega_i^{(2)})it_2}}{(\pm\omega_O \pm \omega_O \pm \omega_X)i(\pm\omega_O)i} \\
& = \hbar X_2^{(2)} \hbar X_2^{(1)} E_L \lambda_X \lambda_X \lambda_O \lambda_O \lambda_x \frac{1}{2} n_i^{(2)} \times \\
& \left( \begin{aligned}
& + \hat{a}_X^- \hat{a}_X^+ \hat{a}_O^- \hat{a}_O^+ \hat{\sigma}_x^{(1)} \hat{\sigma}_\pm^{(2)} \hat{a}_x^\pm e^{\pm \phi_i^{(2)} i} \frac{e^{(\pm\omega_x \pm 2\varepsilon_2 \pm \omega_i^{(2)})it_2}}{(+\omega_X)i(+\omega_O)i} + \hat{a}_X^+ \hat{a}_X^- \hat{a}_O^+ \hat{a}_O^- \hat{\sigma}_x^{(1)} \hat{\sigma}_\pm^{(2)} \hat{a}_x^\pm e^{\pm \phi_i^{(2)} i} \frac{e^{(\pm\omega_x \pm 2\varepsilon_2 \pm \omega_i^{(2)})it_2}}{(-\omega_X)i(+\omega_O)i} \\
& + \hat{a}_X^- \hat{a}_X^+ \hat{a}_O^+ \hat{a}_O^- \hat{\sigma}_x^{(1)} \hat{\sigma}_\pm^{(2)} \hat{a}_x^\pm e^{\pm \phi_i^{(2)} i} \frac{e^{(\pm\omega_x \pm 2\varepsilon_2 \pm \omega_i^{(2)})it_2}}{(+\omega_X)i(-\omega_O)i} + \hat{a}_X^+ \hat{a}_X^- \hat{a}_O^- \hat{a}_O^+ \hat{\sigma}_x^{(1)} \hat{\sigma}_\pm^{(2)} \hat{a}_x^\pm e^{\pm \phi_i^{(2)} i} \frac{e^{(\pm\omega_x \pm 2\varepsilon_2 \pm \omega_i^{(2)})it_2}}{(-\omega_X)i(-\omega_O)i}
\end{aligned} \right) \\
& = \hbar X_2^{(2)} \hbar X_2^{(1)} E_L \frac{\lambda_X \lambda_X \lambda_O \lambda_O}{(+\omega_X)i(+\omega_O)i} \lambda_x \frac{1}{2} n_i^{(2)} \hat{\sigma}_x^{(1)} \hat{\sigma}_\pm^{(2)} \hat{a}_x^\pm e^{\pm \phi_i^{(2)} i} e^{(\pm\omega_x \pm 2\varepsilon_2 \pm \omega_i^{(2)})it_2} \\
& = \hbar X_2^{(2)} \hbar X_2^{(1)} E_L (4E_{JX} E_{JO})^{-1} \lambda_x \frac{1}{2} n_i^{(2)} \hat{\sigma}_x^{(1)} \hat{\sigma}_\pm^{(2)} \hat{a}_x^\pm e^{\pm \phi_i^{(2)} i} e^{(\pm\omega_x \pm 2\varepsilon_2 \pm \omega_i^{(2)})it_2}
\end{aligned}$$

The coupling terms  $I_1 \int_0^t I_3 dt \int_0^t I_2 dt$  and  $I_2 \int_0^t I_3 dt \int_0^t I_1 dt$  are discarded. The pulses with  $\omega_2^{(2)}$ ,  $\omega_1^{(2)}$  excite the resonant JC coupling and AJC coupling respectively. So, the coupling between momentum and spin in the x direction is shown as  $H_{I3x} = \frac{1}{2} \hbar X_2^{(1)} \hbar X_2^{(2)} E_L (E_{JO} E_{JX})^{-1} \lambda_x n_x \hat{\sigma}_x^{(1)} \hat{\sigma}_x^{(2)} i(\hat{a}_x^+ - \hat{a}_x^-)$

The coupling between momentum and spin in the y direction can be obtained by the iteration where

$$\begin{aligned}
I_1 &= -\hbar X_2^{(1)} \hat{\sigma}_x^{(1)} (\lambda_O \hat{a}_O^+ e^{+\omega_O it} + H.C) (\frac{1}{2} n_i^{(1)} e^{+i(\omega_i^{(1)} t + \phi_i^{(1)})} + H.C) , \\
I_2 &= +\hbar X_2^{(2)} (\hat{\sigma}_+^{(2)} e^{+2\varepsilon_2 it} + H.C) (\lambda_Y \hat{a}_Y^+ e^{+\omega_Y it} + H.C) (\lambda_O \hat{a}_O^+ e^{+\omega_O it} + H.C) , \\
I_3 &= -E_L (\lambda_y \hat{a}_y^+ e^{+\omega_y it} + H.C) (\lambda_Y \hat{a}_Y^+ e^{+\omega_Y it} + H.C) .
\end{aligned}$$

The pulses with  $\omega_1^{(1)}$ ,  $\omega_2^{(1)}$  excite the resonant JC coupling and AJC coupling respectively. So, the coupling between momentum and spin in the y direction is shown as  $H_{I3y} = \frac{1}{2} \hbar X_2^{(1)} \hbar X_2^{(2)} E_L (E_{JO} E_{JY})^{-1} \lambda_y n_y \hat{\sigma}_x^{(1)} \hat{\sigma}_y^{(2)} i(\hat{a}_y^+ - \hat{a}_y^-)$

The coupling between momentum and spin in the z direction can be obtained by the iteration where

$$\begin{aligned}
I_1 &= -\hbar X_2^{(1)} \hat{\sigma}_x^{(1)} (\lambda_Z \hat{a}_Z^+ e^{+\omega_Z it} + H.C) (\lambda_O \hat{a}_O^+ e^{+\omega_O it} + H.C) , \\
I_2 &= +\hbar Z_2^{(2)} \hat{\sigma}_z^{(2)} (\lambda_O \hat{a}_O^+ e^{+\omega_O it} + H.C) (\frac{1}{2} n_i^{(2)} e^{+i(\omega_i^{(2)} t + \phi_i^{(2)})} + H.C) , \\
I_3 &= -E_L (\lambda_z \hat{a}_z^+ e^{+\omega_z it} + H.C) (\lambda_Z \hat{a}_Z^+ e^{+\omega_Z it} + H.C) .
\end{aligned}$$

The pulse with  $\omega_3^{(2)}$  excite the resonant JC coupling and AJC coupling respectively. So, the coupling between momentum and spin in the z direction is shown as  $H_{I3z} = \frac{1}{2} \hbar X_2^{(1)} \hbar Z_2^{(2)} E_L (E_{JO} E_{JZ})^{-1} \lambda_z n_z \hat{\sigma}_x^{(1)} \hat{\sigma}_z^{(2)} i(\hat{a}_z^+ - \hat{a}_z^-)$ .

In 2+1D, all items are same as that in 3+1D, except  $H_{I3z} = 0$ . In 1+1D, the first order approximation is the same as that in 3+1D. The second order approximation represents the resonant coupling term between the flux qubit and phase qubit. It can be obtained by iteration of  $H_{I2} = \sum I_k \int_0^{t_1} I_m dt_2$ , where  $k, m = 1, 2$  and  $k \neq m$ .

$$\begin{aligned}
I_1 &= \hbar X_2 \hat{\sigma}_x (\lambda_X \hat{a}_X^+ e^{+\omega_X it} + H.C) (\frac{1}{2} n_i e^{i(\omega_i t + \phi_i)} + H.C) , \\
I_2 &= -E_L (\lambda_x \hat{a}_x^+ e^{+\omega_x it} + H.C) (\lambda_X \hat{a}_X^+ e^{+\omega_X it} + H.C) .
\end{aligned}$$

It is shown as  $H_{I2} = \frac{1}{2} \hbar X_2^{(1)} E_L E_{JX}^{(-1)} \lambda_x n_1 \hat{\sigma}_x i(\hat{a}_x - \hat{a}_x^+)$ .